A central control circuit for encoding perceived food value

Article (Published Version)

NEUROPHYSIOLOGY

A central control circuit for encoding perceived food value

Michael Crossley, Kevin Staras*†, György Kemenes*

Hunger state can substantially alter the perceived value of a stimulus, even to the extent that the same sensory cue can trigger antagonistic behaviors. How the nervous system uses these graded perceptual shifts to select between opposed motor patterns remains enigmatic. Here, we challenged food-deprived and satiated *Lymnaea* to choose between two mutually exclusive behaviors, ingestion or egestion, produced by the same feeding central pattern generator. Decoding the underlying neural circuit reveals that the activity of central dopaminergic interneurons defines hunger state and drives network reconfiguration, biasing satiated animals toward the rejection of stimuli deemed palatable by food-deprived ones. By blocking the action of these neurons, satiated animals can be reconfigured to exhibit a hungry animal phenotype. This centralized mechanism occurs in the complete absence of sensory retuning and generalizes across different sensory modalities, allowing food-deprived animals to increase their perception of food value in a stimulus-independent manner to maximize potential calorific intake.

INTRODUCTION

Hunger is a potent regulator of animal behavior. Periods of food deprivation can increase risky decision-making, for example, ignoring potential threats in the environment (*1*–*6*) or ingesting potentially harmful food (*7*–*9*). In the latter example, animals must make dynamic decisions about the cost-benefit of food intake relative to their motivational state and select an appropriate behavior; in some cases, the complete reversal of the motor pattern, from ingestion to rejection. How the nervous system encodes internal state, makes decisions about the perceived value of a stimulus, and selects between alternative behavioral responses by motor network reconfiguration are key questions in neurobiology.

Previous studies have demonstrated that hunger state can modulate behavioral responsiveness to a stimulus by influencing sensory pathways (*8*–*12*). Although this provides an efficient tuning mechanism for generating simple graded changes in a particular behavior, whether it could underlie more complex decisions resulting in complete behavioral reversal is unknown. A second possibility, raised by the observation that in both vertebrates and invertebrates, ingestion and egestion are driven by a single CPG (central pattern generator) (*13*, *14*), is that the control switch is central, not peripheral. In this case, motivational state would act on the pattern generator or a connected higher-order network directly, to select the appropriate behavior. This type of central control switching mechanism would endow the system with the ability to generalize behavioral selection to multiple stimuli without the need to retune all the sensory pathways that mediate them.

Here, we examine these possibilities using the freshwater snail *Lymnaea*, one of the best-characterized models for studying feeding control and its neural mechanisms (*15*). This animal generates definable ingestion and egestion behaviors using a simple three-neuron CPG that drives motoneurons and, in turn, a highly complex feeding musculature consisting of 46 muscles (*15*). Moreover, the neurons are large, morphologically consistent, and reidentifiable, and multiple cells can be recorded and manipulated simultaneously using intracellular recording approaches. Critically, the animal's metabolic state is retained in the isolated nervous system (*16*, *17*), allowing the network mechanisms involved in state-dependent feeding decisions to be fully interrogated at a cellular and molecular level. This system therefore offers an attractive entry point for elucidating fundamental mechanisms that encode changes in motivational state and direct the expression of relevant animal behavior.

A forced-choice paradigm was used to demonstrate that a single potential food stimulus drives mutually exclusive behaviors, either ingestion or egestion, that depends on the hunger state of the animal. Using in vivo and in vitro approaches, we show that this behavioral selection uses a higher-order switch mechanism acting directly on the feeding network to drive a motivational state–dependent choice, without sensory retuning. This is achieved by activity in hunger state–encoding dopaminergic interneurons, which reconfigure the feeding network to bias satiated animals toward the rejection of stimuli deemed palatable by food-deprived ones. We also show that this higher-order control permits generalization across different input modalities. In this way, according to its hunger state, an animal can universally adjust the level of risk it is prepared to accept when deciding whether to consume ambiguous material that has food-like cues. Our study reveals a central neuronal switch mechanism that endows the animal with the advantageous ability to make adaptive choices regarding food intake within its highly unpredictable sensory habitat.

RESULTS

Circuit-level expression of mutually exclusive feeding behaviors

Lymnaea can perform two types of feeding behavior, ingestion and egestion, which serve opposing functions. Both behaviors use the same feeding structures (mouth, buccal mass, and radula) (Fig. 1, A and B) and are therefore mutually exclusive. Application of an appetitive stimulus to the lips (lettuce or sucrose) elicits ingestion bites (Fig. 1, A and B, top panels, and movie S1), whereas application of an aversive stimulus (pinch to the esophagus) triggers egestion where the movement of key feeding structures is reversed (Fig. 1B, bottom panels, and movie S2).

Sussex Neuroscience, School of Life Sciences, University of Sussex, Brighton BN1 9QG, UK.
*Joint senior authors.
†Corresponding author. Email: k.staras@sussex.ac.uk

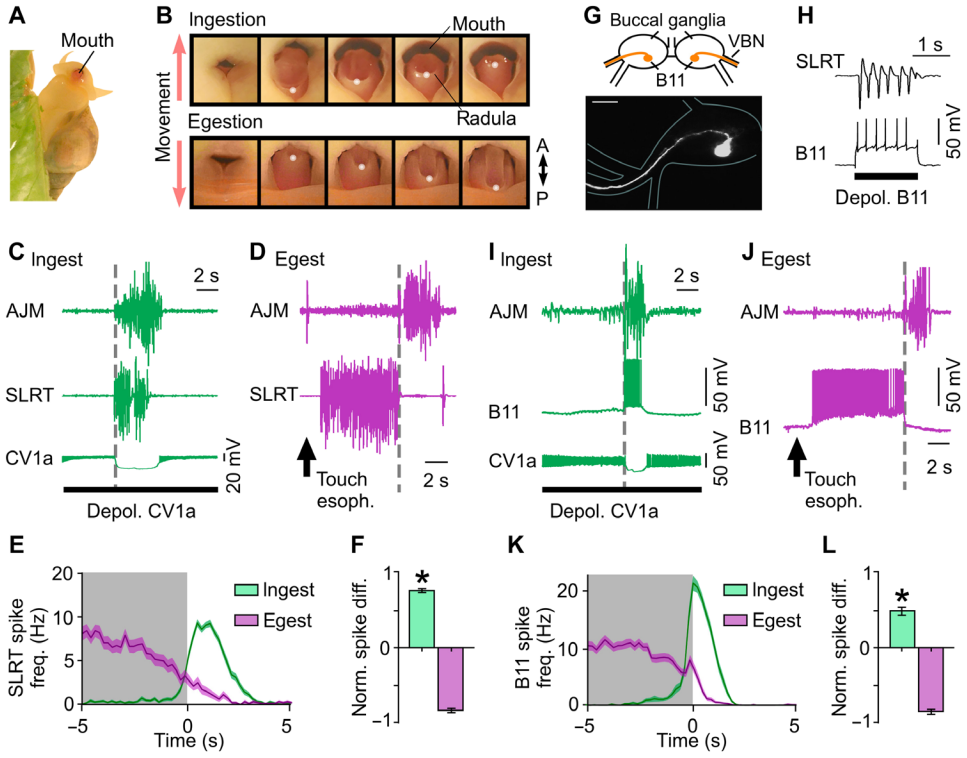

Fig. 1. In vitro correlates of ingestion and egestion behavior. (**A**) *Lymnaea* biting at water surface. (**B**) Mouth movements during ingestion or egestion. White dots indicate the distal tip of the radula tracked in analysis. (**C** and **D**) AJM and SLRT activity in an in vitro preparation during an ingestion cycle after CV1a depolarization (C) and an egestion cycle after touch to the esophagus (D). Gray dashed lines represent the onset of burst of activity on AJM. (**E**) Average frequency of SLRT activity during ingestion (green) ($n = 105$ cycles, 10 preps) and egestion (purple) ($n = 51$ cycles, 8 preps). Line and shading show means ± SEM. (**F**) Normalized difference score of SLRT activity after versus before AJM activity onset with significant difference between ingestion (0.77 ± 0.05) and egestion (−0.83 ± 0.05. unpaired *t* test, $^*P < 0.0001$). Data are shown as means ± SEM. (**G**) Morphology and schematic of B11 motoneuron in the buccal ganglia after iontophoretic dye filling showing single projection leaving ganglion via ventral buccal nerve (VBN) toward buccal mass and SLRT muscle. Morphology was confirmed in $n = 3$ cells. Scale bar, 100 μM. (**H**) Spikes artificially triggered in B11 cause 1:1 activity on SLRT muscle. (**I** and **J**) B11 and AJM activity during ingestion (I) and egestion (J) cycles. (**K**) Average B11 spike frequency during ingestion (green) ($n = 69$ cycles, 9 preps) and egestion (purple) ($n = 78$ cycles, 10 preps) cycles. Line and shading are means ± SEM. (**L**) Normalized difference scores of B11 activity after versus before AJM activity onset showed a significant difference between ingestion (0.49 ± 0.05) and egestion (−0.87 ± 0.03, unpaired *t* test, $^*P < 0.0001$). Data are shown as means ± SEM.

To confirm that this opposed behavioral expression was the consequence of a reversal of the motor control patterns in vitro, we carried out experiments in which we co-recorded from two key radula muscles, the anterior jugalis muscle (AJM) and the supralateral radula tensor (SLRT) muscle (*18*) in a reduced preparation consisting of the central nervous system (CNS) attached to the buccal mass via buccal nerves (see Materials and Methods). Cycles evoked by the command-like interneuron CV1a, an established part of the food-signaling pathway (see fig. S1, A and B) (*19*), or by appetitive stimuli applied to the lips produced a single burst of synchronized activity per cycle in both muscles (Fig. 1, C, E, and F, and fig. S1C). By contrast, egestion behavior, evoked by tactile stimulation of the esophagus, an aversive stimulus (see fig. S1B and Materials and Methods), produced highly asynchronous muscle activity, with SLRT activation preceding AJM (Fig. 1, D to F). As such, differential AJM/SLRT activity expression provides a robust in vitro correlate of ingestion/egestion. Next, we looked for neurons in the CNS that could underlie these opposing muscle activity patterns. Our search identified a new type of motoneuron, B11 (Fig. 1, G and H), which both projected to SLRT and robustly activated it in a 1:1 manner (see Materials and Methods for further details). Furthermore, B11 activity mirrored SLRT activity in both ingestion and egestion cycles (Fig. 1, I to L), showing in-phase activity with the AJM during ingestion cycles but out-of-phase activity during esophageal-activated egestion cycles. As such, B11 is differentially recruited in the two different behaviors, and its activity provides an important central readout of ingestion/egestion expression in vitro.

Choice between ingestion and egestion depends on hunger state

Two opposed behaviors with known neural correlates provide a powerful system to examine the effects of hunger state on behavioral selection. To investigate this, we devised a type of forced-choice paradigm where animals in different motivational states are made to choose between ingestion and egestion behaviors based on the presence of a single type of stimulus. Animals were in one of two states, either fed (food available ad libitum) or food deprived (4 days starved), and were tested for their behavioral response to a tactile stimulus with food-like properties (*17*). In both groups, this stimulus was presented to the mouth as the animal performed an ingestion bite. The radula movement that followed was then classified as either ingestive or egestive, providing a readout of the animal's judgment regarding the potential value of the stimulus. In fed animals, the tactile stimulus evoked net egestive responses, while predominantly ingestive responses were

recorded in food-deprived animals (Fig. 2, A and B). Thus, a single stimulus can elicit one of two mutually exclusive behaviors depending on hunger state: Fed animals perceive the stimulus as inedible, while their food-deprived counterparts initiate ingestive feeding responses.

Next, we tested whether food deprivation is associated with a generalized shift in the state of the feeding network resulting in a switch from egestion to ingestion. As a readout of network state, we used the occasional spontaneous cycles recorded in vitro and classified them as ingestion or egestion patterns based on B11 versus AJM activity (Fig. 2, C and D). Notably, we found that preparations from fed animals were highly biased toward egestion activity, while hungry animals were associated with ingestive patterns (Fig. 2, E and F). We reasoned that this might be explained by an inability of hungry animal preparations to generate egestion cycles at all. To test this, we recorded their B11 responses to esophageal stimulation (fig. S2A) and demonstrated that egestive responses occurred at the same level as observed in fed animals (food deprived, $n = 8$, -0.8 ± 0.06; fed, $n = 10$, -0.87 ± 0.03; normalized difference scores, unpaired t test, $P > 0.05$; see Fig. 1 legend for detail of measurement). We further tested how different levels of food deprivation affected the network state by recording in vitro cycles in 1-, 2-, and 3-day food-deprived preparations (fig. S2B). We observed a trend toward ingestion from 1 day of food deprivation, which reached significance by 3 days versus fed preparations (fig. S2, B and C). Thus, during periods of food deprivation, there is a progressive shift in the state of the feeding network from egestion toward ingestion, presumably associated with a motivational state–dependent change in the central circuits driving these two opposing behaviors.

Higher-order interneurons encode hunger state and select motor patterns

Next, we carried out an extensive characterization of the CNS to identify elements that might drive this hunger state–dependent decision-making circuit (see Materials and Methods). In particular, our search identified a pair of buccal to cerebral interneurons (Fig. 3A) with key characteristics consistent with this function and therefore termed pattern reversing neurons (PRNs). First, activating the egestion pathway in vitro elicited a strong burst of spikes in a PRN, which coincided with B11 activity before AJM activity (Fig. 3B). Moreover, at the onset of the retraction phase, activity in PRN and B11 both ceased. Second, during ingestion cycles, PRN showed no spiking activity (fig. S3A), indicating that it was selectively active during egestion cycles. Third, artificial activation of a single PRN was sufficient to drive exclusively egestive motor programs (Fig. 3C and fig. S3B), and there was no significant difference between PRN-driven cycles and sensory-triggered egestion (PRN, $n = 8$, -0.77 ± 0.04; normalized difference score, unpaired t test, $P > 0.05$). Likewise, CV1a, a driver of ingestive feeding cycles, exhibited no activity during PRN-driven cycles (fig. S3C). To ascertain whether PRN played a role in the motivational state–dependent biasing of motor pattern selection, we recorded PRN activity during spontaneous cycles in preparations from fed and food-deprived animals. We found that these cells exhibited significantly higher firing rates per cycle and significantly more activity cycles in total, in fed versus food-deprived preparations (Fig. 3, D to F). Together, these results demonstrate that a key central control element of the egestion network is in a relative upstate in fed preparations compared with their food-deprived counterparts. Next, we tested whether PRN activity was the source of the bias toward egestion patterns in fed preparations by inhibiting these cells during cycles. We found that hyperpolarizing both

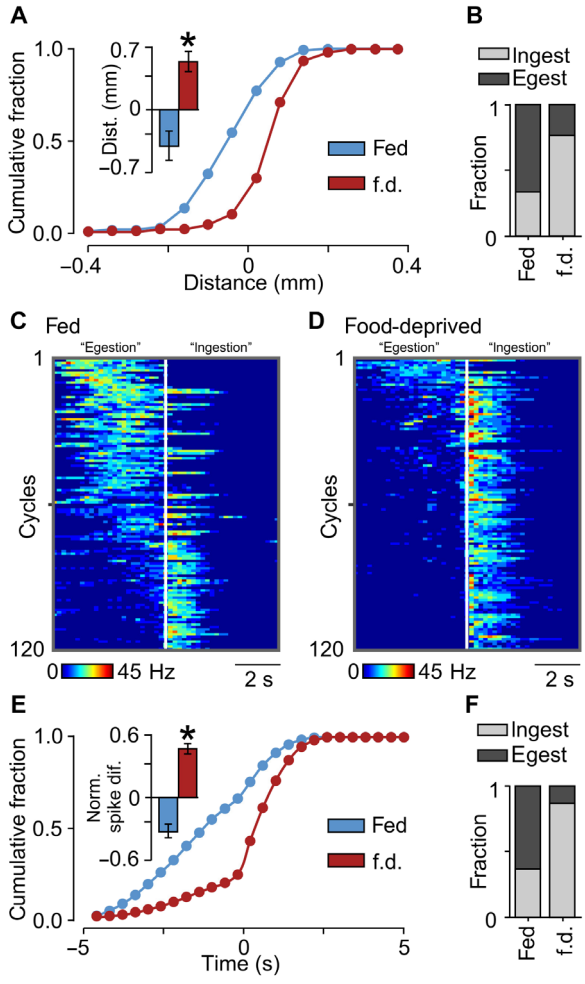

Fig. 2. Choice between ingestion and egestion depends on hunger state. (**A**) Cumulative frequency plot of radula movements in response to tactile probe with food-like properties from fed and food-deprived (f.d.) animals. Bar chart of behavioral response to tactile probe shows a significant difference in radula movements between fed (-0.41 ± 0.17 mm, $n = 18$) and food-deprived (0.55 ± 0.12 mm, $n = 21$) animals (Mann-Whitney U test, $P < 0.0001$). Data are shown as means ± SEM. (**B**) Comparison of fraction of ingestion and egestion bites in response to tactile stimulus with significant difference between fed and food-deprived responses (Fisher's exact test, $P < 0.0001$). (**C** and **D**) Heatplots of B11 activity in multiple trials during in vitro cycles from fed (C) and food-deprived (D) preparations. White lines represent onset of AJM burst. Data are ordered from high to low activity before AJM onset. (**E**) Cumulative frequency plot of B11 activity during cycles from fed and food-deprived preparations. Bar chart showing normalized B11 spike frequency before versus after AJM burst onset ($n = 120$ cycles from 12 preparations for both conditions) showing a significant difference between fed (-0.33 ± 0.11) and food-deprived (0.47 ± 0.1) cycles (unpaired t test, $^*P < 0.0001$). (**F**) Comparison of the fraction of ingestion and egestion cycles. There was a significant difference between fed and food-deprived preparations (Fisher's exact test, $P < 0.0001$).

PRNs alone was sufficient to switch fed preparations from an egestion to ingestion pattern (Fig. 3G). Notably, preventing somatic spikes in both PRNs did not block esophageal-driven egestion (fig. S3F), suggesting that while other elements are involved in the basic ability to egest, PRN has a critical hunger state–specific function. Thus, we conclude that these pivotal command-like interneurons encode in vitro hunger state, serving as a central switch mechanism for motor pattern selection.

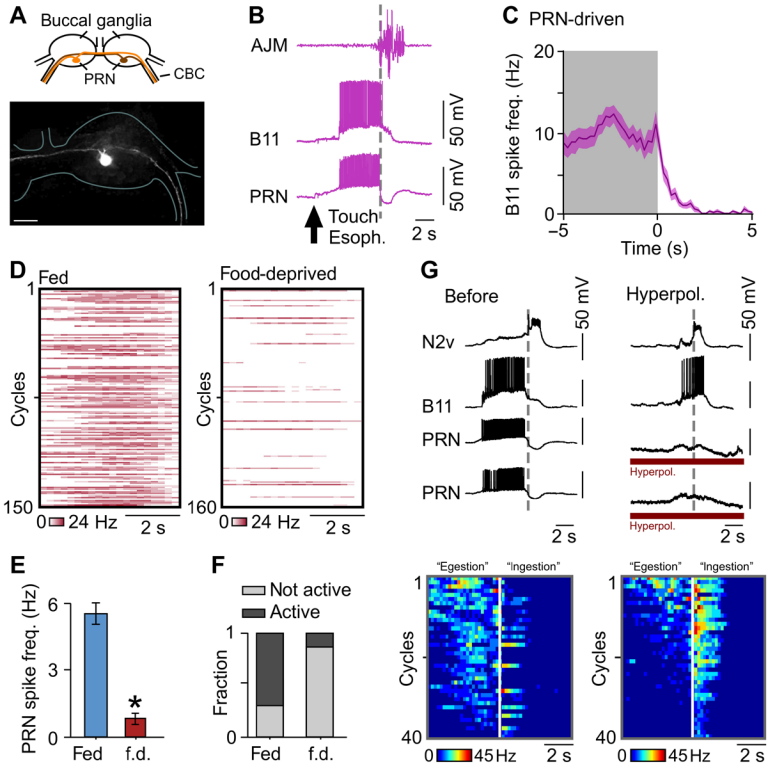

Fig. 3. PRN encodes hunger state and drives network reconfiguration. (**A**) Morphology of PRNs via iontophoretic dye filling demonstrating cerebral buccal connective (CBC) projection, confirmed in $n = 6$ cells. Scale bar, 100 μM. (**B**) Trace of PRN activity during esophageal-driven egestion, co-recorded with B11 and AJM. PRN is active in phase with B11 but not AJM. Gray dashed lines show onset of AJM burst. (**C**) Average spike frequency of B11 activity during PRN-driven cycles (see fig. S3B) ($n = 36$ cycles, eight preps). Line and shading are means ± SEM. (**D**) Heatplots of PRN firing rates during in vitro cycles in fed (left) ($n = 150$ cycles, 15 preps) and food-deprived (right) ($n = 160$ cycles, 16 preps) preparations. (**E** and **F**) Statistical analysis. Fed preparations had more PRN activity per cycle (unpaired t test, $^*P < 0.0001$) and more active cycles (Fisher's exact test, $P < 0.0001$) than food-deprived in these nonstimulated preparations. Data are shown as means ± SEM. (**G**) Representative traces of an in vitro egestion cycle from fed preparation (left). B11 is only active in the protraction phase (see fig. S3, D and E). Hyperpolarizing both PRNs switches B11 activity to ingestion-like pattern (right). Gray dashed lines show retraction phase onset. Heatplots of B11 activity before (left) and during (right) PRN hyperpolarization are shown. White line shows onset of AJM burst. Data are ordered from high to low ($n = 40$ cycles, four preps) with significant B11 difference score before versus during PRN hyperpolarization (before: −0.62 ± 0.06; during: 0.4 ± 0.15, paired t test, $P = 0.002$).

Switching from a satiated to a hungry phenotype in vitro and in vivo

To test whether PRNs account for behavioral selection in vivo, we first identified the transmitter used by these cells to drive egestion. Previous mapping studies have revealed a single pair of unidentified dopaminergic neurons on the ventral surface of the buccal ganglia (*20*, *21*), and we hypothesized that these might be PRNs. Electrophysiology and double-labeling experiments using Alexa Fluor and dopamine antibody staining supported this idea (Fig. 4A). Moreover, experiments showed that the strong PRN→B11 monosynaptic excitatory connection (Fig. 4B, left, and fig. S4, A and B), which accounts for B11 activation during egestion cycles, was blocked with the D2 receptor antagonist, sulpiride ($n = 9$) (Fig. 4B, right, and fig. S4C). Thus, we concluded that dopamine is PRN's transmitter. We further tested whether the animal's hunger state modulated the strength of the PRN→B11 connection, but found no significant difference (fig. S4, D and E). We next examined whether sulpiride application could mimic the modulation of motor program selection in fed preparations seen when PRN activity is suppressed (see Fig. 3G). Specifically, we recorded spontaneous cycles on B11 and AJM in fed preparations before and after bath application of sulpiride to the CNS (Fig. 4C). As expected, egestion cycles predominated in the pretreatment condition, but following sulpiride application, we observed a notable change in cycle expression, with a switch to almost exclusively ingestive cycles (Fig. 4, C to E). Therefore, sulpiride can reconfigure the network state from egestion to ingestion in vitro. As before, we demonstrated that this was not explained by an inability of the feeding system to generate egestion cycles at all when sulpiride treated; tactile stimulation of the esophagus was still able to drive egestion cycles in the presence of the blocker (fig. S4F). Together, this suggests that sulpiride application in vitro inhibits PRN's state-dependent control pathway and biases the preparation toward the selection of ingestion cycles.

Next, we investigated whether the same pharmacological intervention could determine behavioral selection in vivo. Fed animals received the same behavioral test as before (see Fig. 2) but were injected with either normal saline or sulpiride before testing. As expected, in saline-injected animals, the tactile stimulus triggered predominantly egestive responses, but notably, in sulpiride-injected animals, responses were ingestive (Fig. 4, F and G). To address the possibility that changes in another parameter of appetitive or consummatory behavior were driving this effect, we characterized the influence of sulpiride on the animal's food searching locomotion (Fig. 4H), appetitive bite sampling

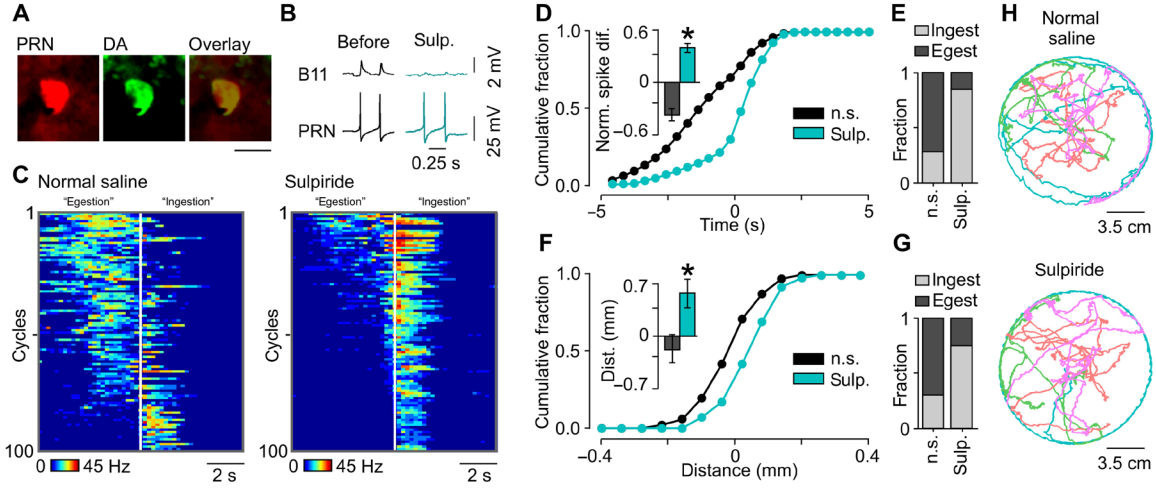

Fig. 4. Switching from satiated to hungry phenotype with dopamine block. (**A**) Double labeling of PRN (iontophoretically filled with Alexa Fluor; left), dopamine (DA) neuron (middle), and overlay (right). Double labeling confirmed in $n = 4$ preparations. Scale bar, 25 μM. (**B**) Evoked spikes in PRN caused 1:1 excitatory postsynaptic potentials (EPSPs) on B11 before (left) and after 10^{-4} M sulpiride application (right). (**C**) Heatplot of B11 activity in vitro in fed preparations before (left) and after (right) sulpiride application. White lines show onset of AJM burst. Data are ordered from high to low activity before AJM onset ($n = 100$ cycles from 10 preps for both conditions). (**D**) Cumulative frequency plot of B11 activity during cycles in normal saline (n.s.) or sulpiride. Bar chart (means ± SEM) of normalized B11 spike frequency before versus after AJM activity shows difference between cycles in normal saline (−0.34 ± 0.14) and sulpiride (0.38 ± 0.07, paired *t* test, $^*P < 0.05$). (**E**) Comparison of fraction of ingestion and egestion cycles for normal saline or sulpiride (Fisher's exact test, $P < 0.0001$). (**F**) Cumulative frequency plot of radula movements in response to tactile probe for animals injected with saline (−0.16 ± 0.17 mm, $n = 16$)– and sulpiride (0.51 ± 0.18 mm, $n = 16$)–injected animals (Mann-Whitney *U* test, $^*P < 0.05$). Data are shown as means ± SEM. (**G**) Comparison of the fraction of ingestion and egestion responses to tactile stimulus (normal saline versus sulpiride; Fisher's exact test, $P < 0.0001$). (**H**) Representative trajectories of saline (top) and sulpiride-injected (bottom) animals ($n = 4$) over 30 min. There was no significant difference in the total distance traversed between groups (saline: 117.1 ± 71.74 cm, $n = 15$; sulpiride: 118.4 ± 65.21 cm, $n = 15$; unpaired *t* test, $P = 0.89$).

behavior, and consummatory behavior in response to sucrose (fig. S4, G and H). None of these parameters showed significant differences between treated and control animals. Thus, sulpiride provides a targeted effect on the motivational state–dependent behavioral selection between ingestion and egestion within the feeding network and effectively switches satiated animals to a hungry phenotype. These results show that PRN encodes hunger state and supports the notion that it acts as a central switch for behavioral selection in vivo.

Sensory retuning is not used for behavioral selection

A previously identified mechanism for encoding hunger state–driven adaptive changes in behavior relies on a retuning of the output gain of sensory input pathways (*22*). To test whether a similar gain control process is also used in behavioral selection in *Lymnaea*, we characterized the sensory pathway that conveys tactile information from the radula to the feeding network. Specifically, we identified a bilaterally located pair of neurons in the buccal ganglia that both projected to the radula structure (Fig. 5, A and B) and responded to brief tactile stimulus with robust activity. We confirmed that these neurons had a primary mechanosensory function by demonstrating that this radula tactile response persisted when chemical synaptic transmission was blocked (fig. S5A). Sensory-driven spikes in these neurons, which we termed radula mechanosensory (RM) cells, evoked large excitatory inputs on the command-like cell vTN, the key neuron type that triggers feeding cycles in the presence of a stimulus during an appetitive bite (Fig. 5C) (*17*). To test whether changes in hunger state caused alterations in the response properties of RMs and, in turn, vTNs, we recorded these cells in fed or food-deprived animal preparations during radula stimulation. Notably, prior feeding state had no influence on the number of spikes elicited in RM cells, their amplitude or their interspike interval in evoked bursts (amplitude: fed, 37.5 ± 3.2 mV; food deprived, 37.2 ± 2.1 mV; Mann-Whitney *U* test, $P = 0.88$; interspike interval: fed, 0.06 ± 0.01 s, food deprived, 0.055 ± 0.004 s; Mann-Whitney *U* test, $P = 0.96$; Fig. 5, C and D). Moreover, there was no effect on the amplitude of excitatory responses recorded on vTN (Fig. 5, C to E). We also ruled out the possibility that modulation of dopamine signaling altered the sensory processing of the tactile stimulus by demonstrating that sulpiride treatment did not change either the RM response or the output to vTN (fig. S5, B to D). Together, these results suggest that the identified central switch mechanism is sufficient for behavioral selection in the absence of sensory retuning.

Central control permits generalization of behavioral choice to multiple cues

Given that the central switch mechanism we have characterized is functioning independently of sensory retuning (Fig. 5), we hypothesized that it might generalize to alternative input stimuli. To test this key idea, we used a behavioral forced-choice paradigm with a different sensory modality stimulus—in this case, a chemical cue [amyl acetate (AA)] applied to the mouth during an ingestive bite—thus ensuring no overlap in sensory processing pathways with our previous paradigm. In fed animals, most of the poststimulus responses were classified as egestion, whereas in food-deprived animals, most were classified as ingestion (Fig. 6, A and B). Thus, the hunger state–dependent alteration in the perceived value of a stimulus and subsequent behavioral selection generalizes to another sensory stimulus. Last, we tested whether intervention with sulpiride was sufficient to bias fed animals toward ingestion in response to AA, replicating our findings with the tactile stimulus paradigm. We found that fed animals injected with sulpiride showed significantly more ingestive responses to AA than

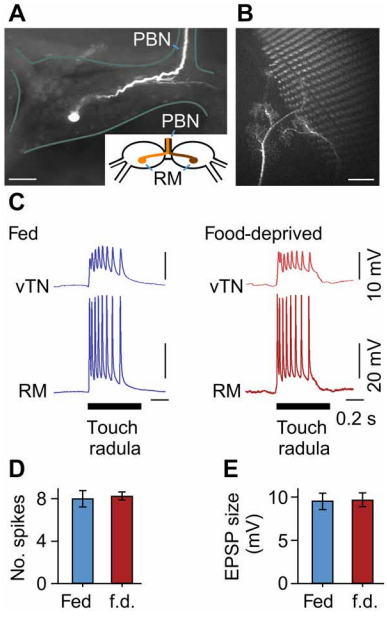

Fig. 5. Hunger state does not alter properties of RM neurons. (**A**) Morphology and schematic of RM neuron in buccal ganglia revealed by iontophoretic dye filling. A single projection leaves the ganglion via the post buccal nerve (PBN) toward the radula. Morphology was confirmed in $n = 4$ preparations. Scale bar, 100 μM. (**B**) Image of a single RM's projection under the toothed radula. Scale bar, 100 μM. (**C**) Representative trace of RM and vTN's response to a tactile stimulus to the radula in fed (blue traces) and food-deprived (red traces) preparations. Touch-induced RM spikes elicit 1:1 EPSPs on vTN. Black bar represents the duration of tactile stimulus (0.5 s). (**D** and **E**) Statistical analysis of RM and vTN response to touch to the radula. There was no significant difference in the number of RM spikes in response to touch between fed ($n = 8$) and food-deprived ($n = 8$) preparations (Mann-Whitney U test, $P > 0.05$) or size of EPSP on vTN (unpaired t test, $P > 0.05$). Error bars represent means ± SEM.

saline-injected animals (Fig. 6, C and D). Therefore, the same drug treatment can alter the animal's perceived value of stimuli of different modalities, providing further strong evidence that PRN acts as a central control switch mechanism for motivational state–dependent behavioral selection.

DISCUSSION

An animal's perception of key features of the environment can change dynamically on the basis of its current internal state. In feeding behavior, this is a critical adaptive mechanism allowing the organism to make cost-benefit decisions about food value versus hunger state, even to the extent that a single stimulus can drive mutually exclusive responses (ingestion or egestion) according to motivation. How the nervous system computes and encodes information about input valence that can lead to the full reversal of behavioral action is not clear. Here, we identify a central control switch in *Lymnaea* that addresses this demand, composed of a dopaminergic interneuron type, PRN, which encodes hunger state, integrates sensory input, and through direct influence on the feeding network, biases an animal toward either ingestion or egestion in response to the same input. Our findings reveal an elegant solution for encoding a complex motivation-driven behavioral reversal with broad relevance for understanding how neural circuits can use parsimonious mechanisms to drive state-dependent peripheral decisions.

Previous examples of motivation-driven behavioral decision-making have revealed a key role for the retuning of sensory pathways (*3*, *22*, *23*). In behavioral responsiveness paradigms in *Drosophila*, hunger increases feeding responses to sucrose (*10*, *24*) and movement toward certain odorants (*11*, *12*) and decreases responsiveness to aversive stimuli (*8*, *9*). Similar fine-tuning of sensory processing in the leech has been implicated in the altered perception of stimuli in other state-dependent decisions (*2*). Likewise, in comparable vertebrate paradigms, hunger state modulates sensory neuron firing properties in response to a stimulus (*23*, *25*). In all cases, for these relatively simple decisions where the animal changes its responsiveness as a means to drive graded increases or decreases in behavior, sensory retuning is apparently an effective solution.

However, these examples contrast with the more complex decision-behavior task we examined in the present study. Here, an animal must switch entirely between two functionally opposed behavioral outputs, suggesting that fundamental differences in the neurobiological mechanisms might be required. Elegant previous work in *Drosophila* has examined how conflicting sensory information is integrated to select between opposed behaviors (*26*). Here, by contrast, we examined how the application of a single stimulus in conjunction with different behavioral states can trigger one of two antagonistic responses. We experimentally ruled out the possibility that the neurons involved in its detection alter either their firing properties or their synaptic connections with command-like interneurons in response to different hunger states. Using an isolated CNS preparation, we demonstrate that hunger state persists in the complete absence of direct sensory activation and biases the configuration of the network. Extending this idea further, we show that, remarkably, this central control switch can also serve to generalize behavioral selection to alternative stimulus modalities. In mice, manipulating the activity in a subset of neurons in the lateral hypothalamus can alter the animal's consummatory responses (*27*, *28*), even to the extent of promoting the ingestion of stimuli of noncalorific content or nonfood stimuli (*4*, *29*). Although not hunger state dependent, these studies demonstrate that, similar to *Lymnaea*, central mechanisms can be used to generalize behavioral selection to multiple sensory stimuli. In view of *Lymnaea*'s complex and varied natural sensory environment, we argue that this provides an efficient mechanism for an animal to set its general level of feeding readiness, regardless of the specific stimuli that it encounters.

How do the homeostatic/endocrine energy control mechanisms in *Lymnaea* compare with those in other systems? In mammals, metabolic hormones such as leptin and insulin have key roles in regulating food intake (*30*, *31*). In particular, food satiation increases the levels of these hormones acting to inhibit hunger state–encoding elements of the feeding circuitry in the hypothalamus (*32*) including NPY (neuropeptide Y)–expressing neurons. The ortholog of NPY in *Drosophila* (dNPF) acts, in part, by altering activity in dopaminergic neurons (*33*). Although an NPY-like peptide is present in *Lymnaea* (LyNPY), evidence suggests that, at least in the short term, it does not affect food intake (*34*). *Lymnaea* also have insulin-like peptides (*35*) as well as a putative leptin-like factor (*34*), which can reduce food intake when administered to food-deprived animals. Similar to other systems, glucose levels are higher in satiated versus hungry *Lymnaea* (*36*), and insulin-containing neurons become active in response to increasing levels of glucose (*37*). It is not yet clear whether the identified dopaminergic PRNs in *Lymnaea* act as direct metabolic sensors. In mice, striatal dopamine levels increase in response to both the sensory and postingestive calorific rewarding effect of sucrose (*38*). These

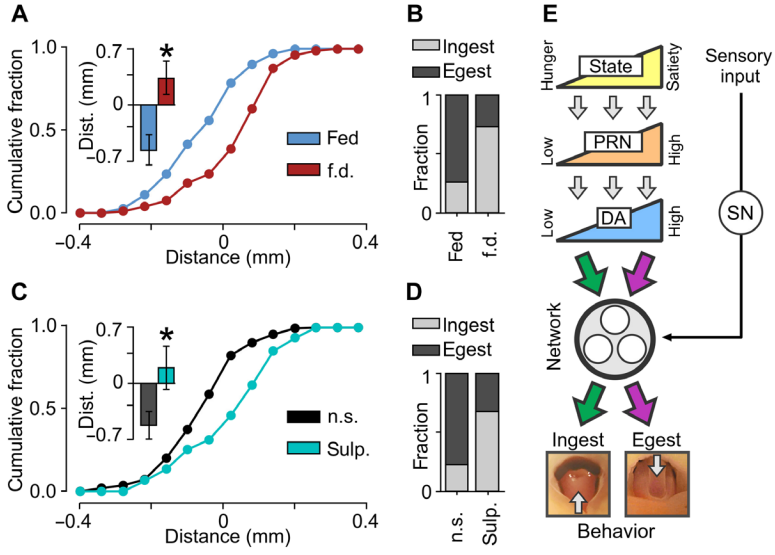

Fig. 6. Hunger state generalizes motor program selection to chemical stimulus. (**A**) Cumulative frequency plot of movements of the radula in response to AA in fed and food-deprived animals. There was a significant difference in the average radula movement in fed (–0.57 ± 0.19 mm, $n = 20$) versus food-deprived (0.34 ± 0.21 mm, $n = 22$) animals (unpaired t test, $^*P < 0.01$). (**B**) Comparison of the fraction of ingestion and egestion responses to AA. There was a significant difference between fed and food-deprived animals (Fisher's exact test, $P < 0.0001$). (**C**) Cumulative frequency plot of movements of the radula in response to AA in animals injected with saline or sulpiride. There was a significant difference in the average radula movement in saline (–0.52 ± 0.17 mm, $n = 18$) compared to sulpiride-injected (0.19 ± 0.28 mm, $n = 18$) animals (unpaired t test, $^*P < 0.05$). (**D**) Comparison of the fraction of ingestion and egestion responses to AA. There was a significant difference between saline- and sulpiride-injected animals (Fisher's exact test, $P < 0.0001$). (**E**) Schematic model depicting sensory-independent biasing of behavioral selection. Changes in hunger state are encoded by changes in activity levels in PRN and, in turn, the levels of dopamine release onto the feeding network. Sensory inputs, via sensory neurons (SN), converge onto the same network, but behavioral selection is based on the network state set by PRN, rather than retuning of these sensory pathways.

striatal dopaminergic neurons, which are able to bias the animal's preference from sucrose to the non-nutritious sucralose (*31*, *38*), act downstream from glucose-sensing hypothalamic neurons (*39*). Possible candidates for a similar type of role in the *Lymnaea* feeding system include glucose-sensitive modulatory neurons (*40*). These cells, acting as metabolic sensors upstream to PRN, could influence membrane properties and thus the excitability of the neuron when glucose levels change with alterations in hunger state.

Our findings suggest a level of network degeneracy (*41*, *42*), where distinct circuit mechanisms can generate the same motor output in a context-dependent manner. The master switch for hunger state–dependent ingestion/egestion behavioral selection is specific to this role, whereas a separate pathway is necessary for esophageal-driven egestion. We found that this purely egestive stimulus was not modulated by the animal's hunger state. This kind of degeneracy, similar to examples in other vertebrate and invertebrate feeding circuits (*43*, *44*), provides both flexibility and hard-wiring of behavior, allowing adaptive responses to a stimulus to be based on the animal's internal state but additionally deprioritizing the hunger-induced bias toward ingestion in response to certain potentially harmful stimuli. Similar mechanisms are used in mammals, where hunger state can alter the perception of inflammatory pain while transient nociceptive pain remains unaffected (*45*). As in *Lymnaea*, this mechanism allows for behavioral adaptation during times of food deprivation, but not at the expense of exposing the animal to potentially life-threatening encounters.

In most systems investigated so far, dopamine signaling has been found to play a role in the processing of a variety of reward-related behaviors (*24*, *33*, *38*, *46*, *47*). It is notable therefore that the central switch neurons, the PRNs, which drive egestion in fed animals, are dopaminergic. Dopamine has been shown to cause network reconfiguration in other systems (*48*, *49*) and to play an important role in shaping behavioral output in a hunger state–dependent manner (*10*, *24*). In these examples, dopamine causes an increase in the positive valuation of a stimulus, whereas in the *Lymnaea* forced-choice paradigm, it seems to lead to a more negative valuation. Notably, this has interesting parallels with important work in *Drosophila* examining food-associated learning circuits where satiety was demonstrated to suppress reward memories through increased activity in a subset of dopaminergic neurons (*33*, *50*). On the basis of the opponent process theory of motivation (*51*), successful avoidance of a potentially dangerous or unpleasant situation [e.g., one that results in the ingestion of a nonpalatable object) may be a reward in its own right (*52*)]. This notion is supported by our finding in *Lymnaea* that dopamine plays an important role in making the decision to reject a potentially harmful stimulus.

Collectively, our findings reveal a fundamental mechanism for changing the perceived value of potential food stimuli in the environment, weighted according to the animal's motivation to feed. A central control mechanism allows the circuit to lower its threshold for promoting ingestion behavior when the animal is hungry, even generalizing across different input modalities, and thus raising the likelihood of successful foraging but at the risk of consuming inedible and potentially harmful foods. In broader behavioral terms, this mechanism would therefore serve to allow an animal to use a riskier feeding strategy when increased hunger state demands it.

MATERIALS AND METHODS

Animal maintenance

All experiments were performed on adult (3 to 4 months old) *Lymnaea stagnalis*. Animals were kept in groups in large holding tanks

containing Cu^{2+}-free water at 20°C on a 12-hour light/12-hour dark regime. The animals were fed lettuce three times a week and a vegetable-based fish food (Tetra Phyll; Tetra Werke, Melle, Germany) twice a week. Animals were transferred to smaller holding tanks before experimenting. Animals were either fed ad libitum or food deprived for 1, 2, 3, or 4 days before either behavioral or electrophysiological experiments.

Preparations and electrophysiological methods

In vitro experiments were carried out using a buccal mass–CNS preparation (*18*) or a radula-CNS preparation (*17*). The buccal mass–CNS preparations was used to record from muscles extracellularly and neurons intracellularly within the CNS. Experiments in Fig. 1 (C and D) were carried out on a preparation that consisted of the entire buccal mass attached to the CNS via the left and right lateral buccal nerves (LBNs) and VBNs, enabling the co-recording of the SLRT muscle and AJMs and intracellular recording of command-like interneuron CV1a (*15*). A small region of the anterior esophagus was kept attached to the CNS by the dorsal buccal nerves (DBNs). A modified version of this preparation was used in Fig. 1 (H to L) and Figs. 2 to 4, which consisted of the buccal mass connected to the CNS via the left LBN and VBN only. During these recordings, the AJM was the only muscle recorded from. This preparation provided greater stability for performing intracellular recordings from motoneurons and interneurons within the buccal ganglia while still providing a readout of the retraction phase. The radula-CNS preparation was used to identify mechanosensory neurons and test whether motivational state altered their response to tactile stimulation of the radula. A 0.5-s tactile stimulus was applied to the radula via a mechanical probe controlled by the ADC (Analogue-to-Digital Converter) board (Micro1401 mk II interface, Cambridge Electronic Design, Cambridge, UK). A lip-CNS preparation was used in fig. S1A to confirm CV1a's responsiveness to appetitive stimuli to the lips. The preparation used is described in detail in (*19*). Saline containing 0.67% sucrose was applied to the lips while recording intracellularly from CV1a. A modified version of this preparation was used in Fig. 1C where the buccal mass was left attached to the CNS similar to that used in Fig. 1 (C and D). This permitted the recording of muscles while applying appetitive stimuli to the lips. Preparations were perfused with normal saline containing 50 mM NaCl, 1.6 mM KCl, 2 mM $MgCl_2$, 3.5 mM $CaCl_2$, and 10 mM Hepes buffer in water. Intracellular recordings were made using sharp electrodes (10 to 40 megohms) filled with 4 M potassium acetate. NL102 (Digitimer Ltd.) and Axoclamp 2B (Axon Instruments, Molecular Devices) amplifiers were used, and data were acquired using a Micro1401 mk II interface and analyzed using Spike2 software (Cambridge Electronic Design, Cambridge, UK). Muscles were recorded using a glass suction electrode. Signals were amplified using an NL104 (20,000 gain) (Digitimer Ltd.) and were low pass (50 Hz) and notch (50 Hz) filtered using NL125/126 filters (Digitimer Ltd.) before they were digitized at a sampling rate of 2 kHz using a Micro1401 mk II interface (Cambridge Electronic Design, Cambridge, UK).

Neurons and muscles recorded

The AJM is a large thick muscle that is involved in the retraction of the buccal mass and the radula/odontophore complex (*18*). Electromyography (EMG) recordings were obtained from the anterior region of this muscle. Most of the activity recorded occurred during the retraction phase (*18*). The SLRT muscles are the largest of the tensor muscles and the bulkiest in the odontophore and have been previously reported to be involved in the retraction phase of a cycle (*18*). EMG recordings were performed on the SLRT on the dorsolateral edges of the odontophore. Command-like interneuron CV1a is located in the cerebral ganglia and was identified by its electrical properties, characteristic location, and ability to drive fictive feeding cycles when artificially depolarized to fire spikes. The N2v neuron is a CPG interneuron located on the ventral surface of the buccal ganglia. It can be identified by its characteristic plateau during the retraction phase of a cycle. Artificial activation of an N2v caused widespread retraction phase activity in many buccal neurons and activity on the AJM. B11 is a newly identified SLRT motoneuron located on the ventral surface of the buccal ganglia. B11 was identified using morphological and electrophysiological criteria. The LBNs and VBNs contain the axons of motoneurons innervating the SLRT. We therefore backfilled these nerves with 5(6)-carboxyfluorescein (5-CF). This reveals a population of putative SLRT motoneurons that we could reidentify in other preparations and test electrophysiologically. Using the preparation consisting of the CNS connected to the SLRT muscle via the lateral and ventral buccal nerves, neurons of interest were impaled, stimulating them while recording extracellular potentials in the SLRT. Spikes in B11 caused contraction of the SLRT muscle and robust 1:1 responses were recorded on the muscle. Touch to the esophagus initiated a barrage of EPSPs on B11, which caused it to spike in the protraction phase of the initiated cycle. To identify candidate members of the egestion network, neurons had to fulfill two criteria: be active in sensory-driven egestion cycles and be sufficient to drive egestion cycles. Projection interneurons are known to be influential in driving patterned activity in *Lymnaea* (*15*). Backfilling the CBC with 5-CF revealed a population of projection neurons, including the paired PRNs. PRN can both drive fictive egestion cycles and is activated during cycles initiated by touch to the esophagus, fulfilling both criteria. PRN also has a 1:1 excitatory connection with B11. RM is a newly identified mechanosensory neuron in the buccal ganglia. Touch to the radula causes somatic spikes in RM, which rise from the baseline and persist in a saline containing zero Ca^{2+} and EGTA, blocking chemical synaptic transmission. The saline contained 35.0 mM NaCl, 1.6 mM KCl, 18.0 mM $MgCl_2$, 2.0 mM EGTA, and 10 mM Hepes buffer in water. vTN was identified due to its location and white color and response to tactile stimulation of the radula (*17*).

In vitro classification of cycles

Artificial activation of CV1a was used to drive fictive ingestion cycles. CV1a is a command-like interneuron that is activated by appetitive sensory stimuli to the lips, which drive ingestion behavior in vivo (see fig. S2A) (*19*). To drive ingestion cycles in vitro, depolarizing current was injected into a single CV1a to elicit spiking until cycles were initiated. These cycles were indistinguishable from those generated by the application of appetitive stimuli to the lips (sucrose). To elicit egestion in vitro, a 1-s tactile stimulus was applied to the region of the esophagus proximal to the point of entry of DBN from the buccal ganglia. The esophagus contains fibers from mechanosensory neurons, which can provide aversive cues to the feeding system in response to overextension of the gut due to an inedible object lodged in the esophagus (*53*). Esophageal stimulation was used instead of a bitter chemical to drive egestion since these chemicals typically produce off-target aversive behaviors, such as defensive withdrawal. The tactile stimulus was applied to the esophagus using a mechanical probe controlled by a TTL (transistor-transistor logic) pulse from the Micro1401 mk II. Large high-frequency AJM activity occurs only in the retraction phase (*18*); therefore, we used this as a constant phase of activity with

which to measure the onset of the retraction phase in all preparations. AJM activity was plotted in 0.2-s bins to aid in identification of the onset of the burst, signaling retraction phase initiation. Activity on the SLRT muscle was measured with respect to the onset of the AJM burst. To analyze the relative activity of SLRT, it was measured 5 s before and 5 s after the AJM burst onset. The number of SLRT events before AJM onset was subtracted from the number of SLRT events after AJM onset and then divided by the total number of events in the 10-s period to gain a normalized difference score. Using this normalized difference score, a positive score represents more activity occurring after AJM onset, and a negative score represents more activity occurring before AJM onset. Based on the analysis of those cycles driven by CV1a and touch to the esophagus, cycles were classified as fictive ingestion cycles if a greater proportion of activity occurred after AJM onset and fictive egestion a greater proportion of activity occurred before the AJM burst onset. The same form of analysis and criteria were used for classifying cycles in which B11 was co-recorded with AJM. B11 spike activity was also plotted as heatplots in Figs. 2 to 4 using MATLAB software. B11 spikes were binned in 0.2-s bins. Data were organized from cycles with most to least activity before AJM onset. To compare the effects of satiety on fictive feeding cycles in vitro, the first 10 spontaneous cycles were analyzed from 12 fed preparations and 12 food-deprived preparations. To test the effects of sulpiride on cycles in fed preparations, the first 10 cycles were recorded in each preparation, and then 10^{-4} M sulpiride in normal saline was perfused on the preparation. The first 10 cycles, which occurred after 10 min of perfusion, were analyzed. PRN spike frequency in fed or food-deprived preparations was recorded in the first 10 spontaneous cycles, which occurred in each preparation. PRN spike frequency was analyzed for 5 s before the onset of the retraction phase and plotted in 0.25-s bins.

Behavioral paradigms

Behavioral paradigm 1

Lymnaea's behavior was observed by placing them in a custom-built behavioral chamber filled with Cu^{2+}-free water. The chamber held the animal on the surface of the water, allowing for the application of sensory stimuli to the mouth of the snail while being able to fully observe movements of the feeding structures. All behavioral experiments were videoed and analyzed using ImageJ software. Animals were left to acclimatize for 10 min before testing. An ingestion bite was triggered by brief application of an appetitive stimulus (lettuce) to the lips of the animal, eliciting a bite response in all animals tested, regardless of hunger state (148 animals). Upon opening of the mouth, either a tactile probe was placed inside or 50 μl of 0.008% AA was applied to the mouth/lips of the animal. The tactile probe consisted of a 1-ml syringe whose tip had been heated and pulled into a fine point. In both conditions, a radula motor program was induced in response to the stimulus. All animals were videoed, and these responses were later analyzed (see below section for details of analysis).

Behavioral paradigm 2

To test whether tactile stimulation of the esophagus elicited ingestion or egestion, an incision was made under the mantle cavity to expose a region of the esophagus, allowing for the mechanical stimulation of the structure with a pair or forceps. Esophageal stimulation was sufficient to elicit an egestion bite even when presented during a period of quiescence. The elicited bite was videoed and analyzed (see below).

Behavioral paradigm 3

To determine the effects of drug injection on animal's locomotion, we tracked animals in a novel environment for 30 min. Briefly, the animals were placed in a 14-cm-diameter petri dish filled with 100 ml of Cu^{2+}-free water. Recording started as soon as they were placed in the arena so as to monitor their initial behavior. Animals were recorded at one frame/s for 30 min. Videos were analyzed using idTracker (*54*), and total distance was traversed compared between groups.

Behavioral paradigm 4

The effects of drug treatment on the animal's food searching behavior in a novel environment were tested by counting the number of appetitive bites during the first 10 min from being placed in a petri dish filled with 100 ml of Cu^{2+}-free water.

Behavioral paradigm 5

The effects of drug treatment on the animal's responsiveness to sucrose were tested by placing the animal in a petri dish filled with 90 ml of Cu^{2+}-free water. Animals were allowed to acclimatize for 10 min, and then 5 ml of water was added to the dish. The number of bites performed was counted for 2 min, and then 5 ml of sucrose (0.33% final solution) was added, and the number of bites performed was counted for 2 min. A feeding score was obtained by subtracting the number of bites in response to water from the number performed in response to sucrose.

Analysis of behavior and characterization of ingestion and egestion in vivo

Biting behavior was videoed at 33 frames/s. The direction of movement of both the radula and the underlying odontophore were measured during the response to either the tactile probe or AA. The video was first rotated so that the animal was aligned with their head to foot in an anterior-to-posterior direction. From the first frame where the radula was visible, it was tracked using ImageJ software in the *y* axis of movement for 10 frames. The last frame was subtracted from the first frame to give a positive or negative direction of movement. A positive score therefore represented a majority anterior movement of the radula, whereas a negative score represented a majority posterior movement. We further measured each of the 10 points the radula was tracked, each point was subtracted from the subsequent point, and cumulative plots of radula movements were generated. We set the criteria to define whether a response was ingestion or egestion based on whether the difference in movement was positive (ingestion) or negative (egestion).

Iontophoretic dye filling of neurons

Neurons were filled with a fluorescent dye, allowing the morphology of the cell to be determined. Microelectrodes were filled with either 5-CF or Alexa Fluor 568 (Molecular Probes). Cells were filled iontophoretically using a pulse generator, which applied regular interval negative square current pulses into the neuron for >30 min. The preparation was then left overnight at 4°C. Images of the neurons were taken using a digital camera (Andor iXon EMCCD) mounted on a Leica stereomicroscope.

Dopamine immunohistochemistry whole-mount staining

CNSs were dissected out in normal saline with 1% sodium metabisulfite (MBS), and neurons were identified and filled with Alexa Fluor 568 as above. The preparations ($n = 4$) were then incubated in 0.25% Protease XIV (Sigma-Aldrich) for 5 min in saline/MBS at room temperature and then washed with saline/MBS. Next, the preparations were fixed for 1 hour in a fixative solution [5% glutaraldehyde in 0.1 M sodium cacodylate buffer (pH 7.4)] at room temperature, then washed in tris/MBS buffer (0.1 M tris base and 0.15 M NaCl), reduced with 1% sodium borohydride in tris/MBS for 10 min, and washed three times with tris/MBS. They were then incubated in 0.1 M phosphate

buffer with 4% Triton X-100 (PBT) plus 1% MBS for 4 hours. Blocking was performed with 1% bovine serum albumin in 0.25% PBT plus 1% MBS overnight at 4°C. The blocking reagent was removed, and the preparations were then incubated with fresh blocking reagent as above but with rabbit anti-dopamine (AB8888, Abcam) at 1:1000 and incubated for 72 hours at 4°C. Three washes with 0.25% PBT followed. The preparations were blocked with 1% normal goat serum in 0.25% PBT plus 1% MBS for 4 hours at room temperature. The blocking reagent was removed, and the preparations were incubated with fresh blocking reagent as above plus goat anti-rabbit Alexa Fluor 488 (A11008, Invitrogen) at 1:100 for 48 hours at 4°C. Three washes with PBS followed. Preparations were then mounted in glycerol mountant on a cavity slide to be imaged.

D2 receptor blocker application in vitro and in vivo

Sulpiride (±) is an effective dopamine antagonist in *Lymnaea*, blocking the effects of dopaminergic neurons and focal application of dopamine (*55*). To test for the effect of sulpiride (±) (Sigma-Aldrich) on the PRN→B11 connection, preparations were bathed in high divalent (HiDi) saline, which increases the threshold for action potentials, acting to reduce polysynaptic connections. HiDi saline was composed of 35.0 mM NaCl, 2 mM KCl, 8.0 mM $MgCl_2$, 14.0 mM $CaCl_2$, and 10 mM Hepes buffer in water. Baseline EPSP size was acquired, then 10^{-4} M sulpiride (±) in HiDi saline was perfused into the bath for 10 min, and EPSP size was recorded again. To test the behavioral effects of sulpiride, animals were injected with 100 µl of 10^{-3} M sulpiride (±) in normal saline. The injected concentration of the drug was diluted ~10-fold by the body fluids of the animal. Control animals were injected with 100 µl of normal saline alone. Animals were left for 2 hours before behavioral tests were carried out.

Quantification and statistical analysis

Data were analyzed using GraphPad Prism 5 (GraphPad Software) and expressed as means ± SEM. Each "*n*" represents an individual preparation, unless stated otherwise in the text. Normality was tested using the D'Agostino and Pearson omnibus normality test. Where data were shown to be normally distributed, two-group statistical comparisons were performed using two-tailed *t* test statistics (either paired or unpaired as stated in the text). Data with more than two groups were first analyzed using a one-way analysis of variance (ANOVA), followed by a Tukey's multiple comparison test. Non-normally distributed data were analyzed using a Mann-Whitney *U* test or Wilcoxon signed-rank test. The comparisons between the percentage of bites/cycles classified as ingestion or egestion were compared using a Fisher's exact test. The significance level was set at $P < 0.05$.

SUPPLEMENTARY MATERIALS

Supplementary material for this article is available at http://advances.sciencemag.org/cgi/content/full/4/11/eaau9180/DC1

Fig. S1. Initiation of ingestion and egestion cycles.
Fig. S2. Increasing periods of food deprivation shift the network state toward ingestion.
Fig. S3. Activity of PRN during ingestion and egestion.
Fig. S4. Sulpiride does not affect other aspects of feeding behavior.
Fig. S5. Sulpiride does not alter RM firing properties.
Movie S1. Ingestion behavior in *Lymnaea*.
Movie S2. Egestion behavior in *Lymnaea*.

REFERENCES AND NOTES

1. S. L. Padilla, J. Qiu, M. E. Soden, E. Sanz, C. C. Nestor, F. D. Barker, A. Quintana, L. S. Zweifel, O. K. Rønnekleiv, M. J. Kelly, R. D. Palmiter, Agouti-related peptide neural circuits mediate adaptive behaviors in the starved state. *Nat. Neurosci.* **19**, 734–741 (2016).
2. Q. Gaudry, W. B. Kristan Jr., Behavioral choice by presynaptic inhibition of tactile sensory terminals. *Nat. Neurosci.* **12**, 1450–1457 (2009).
3. D. D. Ghosh, T. Sanders, S. Hong, L. Y. McCurdy, D. L. Chase, N. Cohen, M. R. Koelle, M. N. Nitabach, Neural architecture of hunger-dependent multisensory decision making in *C. elegans*. *Neuron* **92**, 1049–1062 (2016).
4. C. J. Burnett, C. Li, E. Webber, E. Tsaousidou, S. Y. Xue, J. C. Brüning, M. J. Krashes, Hunger-driven motivational state competition. *Neuron* **92**, 187–201 (2016).
5. A. Filosa, A. J. Barker, M. Dal Maschio, H. Baier, Feeding state modulates behavioral choice and processing of prey stimuli in the zebrafish tectum. *Neuron* **90**, 596–608 (2016).
6. L. B. Bräcker, K. P. Siju, N. Varela, Y. Aso, M. Zhang, I. Hein, M. L. Vasconcelos, I. C. Grunwald Kadow, Essential role of the mushroom body in context-dependent CO_2 avoidance in *Drosophila*. *Curr. Biol.* **23**, 1228–1234 (2013).
7. R. Gillette, R.-C. Huang, N. Hatcher, L. L. Moroz, Cost-benefit analysis potential in feeding behavior of a predatory snail by integration of hunger, taste, and pain. *Proc. Natl. Acad. Sci. U.S.A.* **97**, 3585–3590 (2000).
8. H. K. Inagaki, K. M. Panse, D. J. Anderson, Independent, reciprocal neuromodulatory control of sweet and bitter taste sensitivity during starvation in *Drosophila*. *Neuron* **84**, 806–820 (2014).
9. E. E. LeDue, K. Mann, E. Koch, B. Chu, R. Dakin, M. D. Gordon, Starvation-induced depotentiation of bitter taste in *Drosophila*. *Curr. Biol.* **26**, 2854–2861 (2016).
10. H. K. Inagaki, S. B.-T. de-Leon, A. M. Wong, S. Jagadish, H. Ishimoto, G. Barnea, T. Kitamoto, R. Axel, D. J. Anderson, Visualizing neuromodulation in vivo: TANGO-mapping of dopamine signaling reveals appetite control of sugar sensing. *Cell* **148**, 583–595 (2012).
11. C. M. Root, K. I. Ko, A. Jafari, J. W. Wang, Presynaptic facilitation by neuropeptide signaling mediates odor-driven food search. *Cell* **145**, 133–144 (2011).
12. K. I. Ko, C. M. Root, S. A. Lindsay, O. A. Zaninovich, A. K. Shepherd, S. A. Wasserman, S. M. Kim, J. W. Wang, Starvation promotes concerted modulation of appetitive olfactory behavior via parallel neuromodulatory circuits. *eLife* **4**, e08298 (2015).
13. J. X. Li, J. X. Maier, E. E. Reid, D. B. Katz, Sensory cortical activity is related to the selection of a rhythmic motor action pattern. *J. Neurosci.* **36**, 5596–5607 (2016).
14. J. Jing, K. R. Weiss, Interneuronal basis of the generation of related but distinct motor programs in *Aplysia*: Implications for current neuronal models of vertebrate intralimb coordination. *J. Neurosci.* **22**, 6228–6238 (2002).
15. P. R. Benjamin, Distributed network organization underlying feeding behavior in the mollusk *Lymnaea*. *Neural. Syst. Circuits* **2**, 4 (2012).
16. K. Staras, I. Kemenes, P. R. Benjamin, G. Kemenes, Loss of self-inhibition is a cellular mechanism for episodic rhythmic behavior. *Curr. Biol.* **13**, 116–124 (2003).
17. M. Crossley, K. Staras, G. Kemenes, A two-neuron system for adaptive goal-directed decision-making in *Lymnaea*. *Nat. Commun.* **7**, 11793 (2016).
18. R. M. Rose, P. R. Benjamin, The relationship of the central motor pattern to the feeding cycle of *Lymnaea stagnalis*. *J. Exp. Biol.* **80**, 137–163 (1979).
19. G. Kemenes, K. Staras, P. R. Benjamin, Multiple types of control by identified interneurons in a sensory-activated rhythmic motor pattern. *J. Neurosci.* **21**, 2903–2911 (2001).
20. K. Elekes, G. Kemenes, L. Hiripi, M. Geffard, P. R. Benjamin, Dopamine-immunoreactive neurones in the central nervous system of the pond snail *Lymnaea stagnalis*. *J. Comp. Neurol.* **307**, 214–224 (1991).
21. L. O. Vaasjo, A. M. Quintana, M. R. Habib, P. A. Mendez de Jesus, R. P. Croll, M. W. Miller, GABA-like immunoreactivity in *Biomphalaria*: Colocalization with tyrosine hydroxylase-like immunoreactivity in the feeding motor systems of panpulmonate snails. *J. Comp. Neurol.* **526**, 1790–1805 (2018).
22. C.-Y. Su, J. W. Wang, Modulation of neural circuits: How stimulus context shapes innate behavior in *Drosophila*. *Curr. Opin. Neurobiol.* **29**, 9–16 (2014).
23. E. Breunig, I. Manzini, F. Piscitelli, B. Gutermann, V. Di Marzo, D. Schild, D. Czesnik, The endocannabinoid 2-arachidonoyl-glycerol controls odor sensitivity in larvae of Xenopus laevis. *J. Neurosci.* **30**, 8965–8973 (2010).
24. S. Marella, K. Mann, K. Scott, Dopaminergic modulation of sucrose acceptance behavior in Drosophila. *Neuron* **73**, 941–950 (2012).
25. A. A. Nikonov, J. M. Butler, K. E. Field, J. Caprio, K. P. Maruska, Reproductive and metabolic state differences in olfactory responses to amino acids in a mouth brooding African cichlid fish. *J. Exp. Biol.* **220**, 2980–2992 (2017).
26. L. P. Lewis, K. P. Siju, Y. Aso, A. B. Friedrich, A. J. Bulteel, G. M. Rubin, I. C. Grunwald Kadow, A higher brain circuit for immediate integration of conflicting sensory information in Drosophila. *Curr. Biol.* **25**, 2203–2214 (2015).
27. J. H. Jennings, R. L. Ung, S. L. Resendez, A. M. Stamatakis, J. G. Taylor, J. Huang, K. Veleta, P. A. Kantak, M. Aita, K. Shilling-Scrivo, C. Ramakrishnan, K. Deisseroth, S. Otte, G. D. Stuber, Visualizing hypothalamic network dynamics for appetitive and consummatory behaviors. *Cell* **160**, 516–527 (2015).
28. E. H. Nieh, G. A. Matthews, S. A. Allsop, K. N. Presbrey, C. A. Leppla, R. Wichmann, R. Neve, C. P. Wildes, K. M. Tye, Decoding neural circuits that control compulsive sucrose seeking. *Cell* **160**, 528–541 (2015).

29. M. Navarro, J. J. Olney, N. W. Burnham, C. M. Mazzone, E. G. Lowery-Gionta, K. E. Pleil, T. L. Kash, T. E. Thiele, Lateral hypothalamus GABAergic neurons modulate consummatory behaviors regardless of the caloric content or biological relevance of the consumed stimuli. *Neuropsychopharmacology* **41**, 1505–1512 (2016).
30. I. S. Farooqi, E. Bullmore, J. Keogh, J. Gillard, S. O'Rahilly, P. C. Fletcher, Leptin regulates striatal regions and human eating behavior. *Science* **317**, 1355 (2007).
31. A. I. Domingos, J. Vaynshteyn, H. U. Voss, X. Ren, V. Gradinaru, F. Zang, K. Deisseroth, I. E. de Araujo, J. Friedman, Leptin regulates the reward value of nutrient. *Nat. Neurosci.* **14**, 1562–1568 (2011).
32. S. Pinto, A. G. Roseberry, H. Liu, S. Diano, M. Shanabrough, X. Cai, J. M. Friedman, T. L. Horvath, Rapid rewiring of arcuate nucleus feeding circuits by leptin. *Science* **304**, 110–115 (2004).
33. M. J. Krashes, S. DasGupta, A. Vreede, B. White, J. D. Armstrong, S. Waddell, A neural circuit mechanism integrating motivational state with memory expression in Drosophila. *Cell* **139**, 416–427 (2009).
34. M. de Jong-Brink, A. ter Maat, C. P. Tensen, NPY in invertebrates: Molecular answers to altered functions during evolution. *Peptides* **22**, 309–315 (2001).
35. A. B. Smit, E. Vreugdenhil, R. H. Ebberink, W. P. Geraerts, J. Klootwijk, J. Joosse, Growth-controlling molluscan neurons produce the precursor of an insulin-related peptide. *Nature* **331**, 535–538 (1988).
36. K. Mita, A. Okuta, R. Okada, D. Hatakeyama, E. Otsuka, M. Yamagishi, M. Morikawa, Y. Naganuma, Y. Fujito, V. Dyakonova, K. Lukowiak, E. Ito, What are the elements of motivation for acquisition of conditioned taste aversion? *Neurobiol. Learn. Mem.* **107**, 1–12 (2014).
37. K. S. Kits, R. C. Bobeldijk, M. Crest, J. C. Lodder, Glucose-induced excitation in molluscan central neurons producing insulin-related peptides. *Pflugers Arch.* **417**, 597–604 (1991).
38. I. E. de Araujo, A. J. Oliveira-Maia, T. D. Sotnikova, R. R. Gainetdinov, M. G. Caron, M. A. Nicolelis, S. A. Simon, Food reward in the absence of taste receptor signaling. *Neuron* **57**, 930–941 (2008).
39. A. I. Domingos, A. Sordillo, M. O. Dietrich, Z. W. Liu, L. A. Tellez, J. Vaynshteyn, J. G. Ferreira, M. I. Ekstrand, T. L. Horvath, I. E. de Araujo, J. M. Friedman, Hypothalamic melanin concentrating hormone neurons communicate the nutrient value of sugar. *eLife* **2**, e01462 (2013).
40. M. Alania, V. Dyakonova, D. A. Sakharov, Hyperpolarization by glucose of feeding-related neurons in snail. *Acta Biol. Hung.* **55**, 195–200 (2004).
41. G. J. Gutierrez, T. O'Leary, E. Marder, Multiple mechanisms switch an electrically coupled, synaptically inhibited neuron between competing rhythmic oscillators. *Neuron* **77**, 845–858 (2013).
42. M. Beverly, S. Anbil, P. Sengupta, Degeneracy and neuromodulation among thermosensory neurons contribute to robust thermosensory behaviors in Caenorhabditis elegans. *J. Neurosci.* **31**, 11718–11727 (2011).
43. J. N. Betley, Z. F. Cao, K. D. Ritola, S. M. Sternson, Parallel, redundant circuit organization for homeostatic control of feeding behavior. *Cell* **155**, 1337–1350 (2013).
44. E. C. Cropper, A. M. Dacks, K. R. Weiss, Consequences of degeneracy in network function. *Curr. Opin. Neurobiol.* **41**, 62–67 (2016).
45. A. L. Alhadeff, Z. Su, E. Hernandez, M. L. Klima, S. Z. Phillips, R. A. Holland, C. Guo, A. W. Hantman, B. C. De Jonghe, J. N. Betley, A neural circuit for the suppression of pain by a competing need state. *Cell* **173**, 140–152.e15 (2018).
46. S. Waddell, Reinforcement signalling in Drosophila; dopamine does it all after all. *Curr. Opin. Neurobiol.* **23**, 324–329 (2013).
47. C.-H. Tsao, C.-C. Chen, C.-H. Lin, H.-Y. Yang, S. Lin, *Drosophila* mushroom bodies integrate hunger and satiety signals to control innate food-seeking behavior. *eLife* **7**, e35264 (2018).
48. E. Marder, Neuromodulation of neuronal circuits: Back to the future. *Neuron* **76**, 1–11 (2012).
49. R. Cohn, I. Morantte, V. Ruta, Coordinated and compartmentalized neuromodulation shapes sensory processing in Drosophila. *Cell* **163**, 1742–1755 (2015).
50. E. Perisse, D. Owald, O. Barnstedt, C. B. Talbot, W. Huetteroth, S. Waddell, Aversive learning and appetitive motivation toggle feed-forward inhibition in the *Drosophila* mushroom body. *Neuron* **90**, 1086–1099 (2016).
51. R. L. Solomon, J. D. Corbit, An opponent-process theory of motivation. I. Temporal dynamics of affect. *Psychol. Rev.* **81**, 119–145 (1974).
52. W. Schultz, Neuronal reward and decision signals: From theories to data. *Physiol. Rev.* **95**, 853–951 (2015).
53. C. J. Elliott, P. R. Benjamin, Esophageal mechanoreceptors in the feeding system of the pond snail, Lymnaea stagnalis. *J. Neurophysiol.* **61**, 727 (1989).
54. A. Perez-Escudero, J. Vicente-Page, R. C. Hinz, S. Arganda, G. G. de Polavieja, idTracker: Tracking individuals in a group by automatic identification of unmarked animals. *Nat. Methods* **11**, 743–748 (2014).
55. N. S. Magoski, L. G. Bauce, N. I. Syed, A. G. Bulloch, Dopaminergic transmission between identified neurons from the mollusk, Lymnaea stagnalis. *J. Neurophysiol.* **74**, 1287–1300 (1995).

Acknowledgments: We thank M. Schofield and P. R. Benjamin for help with the dopamine staining. **Funding:** This work was funded by the Biotechnology and Biological Research Council (BBSRC/BB/H009906/1 and BBSRC/BB/P00766X/1) to G.K. and M.C. K.S. was supported by funding from BBSRC/BB/K019015/1. **Author contributions:** M.C., K.S., and G.K. conceived and designed the experiments. M.C. performed the experiments. M.C. and K.S. analyzed the data and made the figures. M.C., K.S., and G.K. wrote the paper. G.K. acquired the funding and was responsible for resources. **Competing interests:** The authors declare that they have no competing interests. **Data and materials availability:** All data needed to evaluate the conclusions in the paper are present in the paper and/or the Supplementary Materials. Detailed numerical data are available on FigShare (DOI: https://doi.org/10.25377/sussex.7133897). Additional data related to this paper may be requested from the authors.

Submitted 27 July 2018
Accepted 24 October 2018
Published 21 November 2018
10.1126/sciadv.aau9180

Citation: M. Crossley, K. Staras, G. Kemenes, A central control circuit for encoding perceived food value. *Sci. Adv.* **4**, eaau9180 (2018).

A central control circuit for encoding perceived food value

Michael Crossley, Kevin Staras and György Kemenes

Sci Adv **4** (11), eaau9180.
DOI: 10.1126/sciadv.aau9180